INTERNATIONAL JOURNAL OF AUTOMOTIVE AND MECHANICAL ENGINEERING
ISSN: 2229-8649 e-ISSN: 2180-1606
VOL. 20, ISSUE 3, 2023, 10695 – 10709
DOI: https://doi.org/10.15282/ijame.20.3.2023.12.0826

RESEARCH ARTICLE

Artificial Neural Network-Based Fault Diagnosis of Gearbox using Empirical Mode Decomposition from Vibration Response

R.R. Mutra[1], D.M. Reddy[1,*], M. Amarnath[2], M.N. Abdul Rani[3,4] , M.A. Yunus[3,4] and M.S.M. Sani[5]

[1]School of Mechanical Engineering, Vellore Institute of Technology, Vellore, Tamil Nadu, 632014, India
[2]Department of Mechanical Engineering, Indian Institute of Information Technology, Design, and Manufacturing, 482005 Jabalpur, India
[3]School of Mechanical Engineering, College of Engineering Universiti Teknologi MARA (UiTM), Shah Alam, 40450, Malaysia
[4]Institute for Infrastructure Engineering and Sustainable Management (IIESM), Universiti Teknologi MARA (UiTM), Shah Alam, 40450, Malaysia
[5]Faculty of Mechanical and Automotive Engineering Technology, Universiti Malaysia Pahang Al-Sultan Abdullah, 26600, Pekan, Pahang Malaysia

ABSTRACT - This paper presents a gearbox defect diagnosis based on vibration behaviour. In order to record the vibration response under various circumstances, an industrial gearbox was used as the basis for an experimental setup. The signals resulting from gear wear were processed using an empirical mode decomposition for two operating time intervals (zero-hour running time and thirty-hour running time). The first three intrinsic mode functions and the corresponding frequency response were detected. The ten statistical parameters most sensitive to gear wear were selected using an evaluation method based on Euclidean distance. Using the identified features, an artificial neural network (ANN) was trained to track the gearbox for the selected future data set. The neural network received its input from the statistical parameters, and its output was the number of gearbox running hours. To achieve faster convergence, the radial basis function and the backpropagation neural network were compared. The superiority of the proposed strategy is demonstrated by comparing the performance of ANN. For monitoring the condition of industrial gears, the proposed strategy is found to be effective and trustworthy.

ARTICLE HISTORY
Received : 16th Feb 2023
Revised : 05th Aug 2023
Accepted : 11th Sept 2023
Published : 11th Oct 2023

KEYWORDS
Fault diagnostics;
Condition monitoring;
Differential gearbox;
Empirical mode;
Decomposition

1.0 INTRODUCTION

Recent advances in information and communication technology (ICT) have equipped modern engineers with the ability to connect devices to the network and track them in real time. Radio Frequency Identification Devices (RFID), developed in the laboratories of Auto-ID in 1999, were the origin of the Internet of Things (IoT). It was later referred to as "the intelligent connectivity for anything, anytime, anywhere" in the 2005 International Telecommunication Union report [1]. This technology enabled the user to collect the required data in real-time from the physical resources with the help of various devices such as RFID, Global Positioning System (GPS), sensors, and scanners. With the advancements in the communication system, the application of IoT is being extended to numerous fields such as healthcare, smart buildings, social security, transportation/distribution, agriculture, smart cities, inventory management, real-time maintenance, etc. A McKinsey Global Institute report estimates that the economic impact of IoT will exceed $11.1 trillion per year by 2025 [2]. Cloud computing is already one of the most important technologies transforming businesses worldwide. The concept of Design Anywhere Manufacture Anywhere (DAMA), which is a plug-and-play approach to cloud manufacturing, is now part of the mainstream in manufacturing [3]. A 5C architecture is proposed for integrating physical systems with advanced cloud computing technology [4]. Enriched maintenance using these techniques can be an important aspect of value creation in the factory. The McKinsey report estimates that maintenance costs can be reduced by 10-40% using these techniques [2]. One can expect a 50 % reduction in machine downtime and a 3 to 5 % reduction in capital investment in equipment. These savings can have a potential economic benefit of $630 billion per year by the end of 2025. To monitor the health of physical systems through the fusion of ICT with best practices, a cloud-based cyber-physical system architecture (CPS) needs to be developed.

Condition-based maintenance (CBM) enables predictive maintenance based on decisions made by detecting abnormal operational conditions. This not only reduces machine downtime but also ensures greater reliability. The three primary processes of CBM are data gathering, data processing, and decision-making on maintenance. Thus, maintenance procedures have changed from an organisation-centric to a customer-centric approach, which has encouraged the growth of prognostics and health monitoring (PHM). This helps to identify invisible patterns of asset deterioration, inconsistencies, and process inefficiencies, leading to improved machine feasibility and, ultimately zero breakdowns [4]. Modern industry is changing rapidly with advances in ICT and predictive analytics. ICT integration with the physical system in close connection, such as the differential gearbox, is referred to as CPS [5]. Gears can not only transmit power or rotary motion between shafts but also provide the necessary angular ratio with incredibly smooth and effective motion transmission. Due to wear, gears lose efficiency over time, making the situation worse. This continuity can lead to loss of production and, eventually, complete breakdown of the entire system. Besides vibrational analysis [6], acoustic

*CORRESPONDING AUTHOR | D. Mallikarjuna Reddy | ✉ dmreddy@vit.ac.in
© The Authors 2023. Published by Universiti Malaysia Pahang Publishing. This is an open access article under the CC BY-NC 4.0 license

emission [7], thermography [8], electrical signature [9], and oil and wear debris analysis [10], vibration analysis is the most extensively used and popular condition monitoring method. In general vibration analysis, experiments are conducted on intentionally damaged and undamaged gears. The gears are artificially damaged by creating cracks of varying severity, the presence of which is reflected in the recorded vibration signals. However, consistent gear wear data reflects the realistic operating condition of the machine and would be more desirable for condition monitoring. Therefore, an approach that collects signal data at different running times may be more reliable and convincing for the industrial environment. Ullah et al. [11] investigated the reduction of contact stresses and better load distribution in the gearbox by optimising the gearing under different operating conditions.

Accurate interpretation of the measured vibration signal under different operational conditions requires deep understanding and expertise. As a result, the vibration data is processed using several signal-processing algorithms to determine which of the acquired data is the most sensitive. Several signal processing techniques, including statistical techniques, time-domain averaging, cepstrum estimation, Wigner–Viller distribution, demodulation [12], independent or principal component analysis cyclo-stationarity analysis, wavelet transforms [13] and EMD [14] have been utilised for signal processing. To overcome the disadvantages of the wavelet transform method, EMD was introduced. Huang et al. [15] introduced this novel method for analysing nonlinear and nonstationary signals in mid-1990s. The Hilbert-Huang transform (HHT), as it is more commonly called, has been praised for its effective and powerful approach to the study of nonstationary and nonlinear time-frequency signal data. EMD and Hilbert spectral analysis are combined to form HHT. The Fast Fourier Transform (FFT) and other wavelet transform decompositions, unlike this unique EMD, do not use specified basis functions. Previously, the upper and lower envelopes of each sighting were determined by cubic splines. The mean of these envelopes was later subtracted from the previously sifted time series. When later studies highlighted the crucial role of the mean curve, research focused on improving EMD. Further work and research proposed a novel decomposition method that combined B-splines with the linear moving mean of the extrema [16]. With the moving mean as the baseline, the EMD algorithm continued in the same way. For the envelope fitting, rational splines were used instead of cubic splines. Intrinsic time scale decomposition (ITD) was also proposed as an alternative to EMD; the effectiveness of EMD for spur gear fault diagnosis was investigated.

IMFs use statistical moments describing the shape of the amplitude distribution of vibration signals data sensitive to energies [17].. Mutra and Srinivas [18] investigated the dynamics of the turbocharger system from the vibration response using Time Domain and Fast Fourier Transforms. Diverse statistical parameters applied to the IMF enhance the fault diagnostic information. The most widely used parameters are kurtosis, crest factor (CF), root mean square (RMS), and skewness due to their simplicity and effectiveness [19–22]. It was reported that more accurate results can be obtained by combining multiple feature parameters for fault diagnosis. However, the use of multiple features makes it difficult for the diagnostic expert to pay attention to each feature because the contradictory values have to be dealt with. In the past, diagnostic experts had considerable difficulty diagnosing faults by simply visually observing the statistical features [23]. This problem has been effectively solved by combining multiple statistical parameters using the pattern recognition technique.

Moreover, this can be an automated, practical, and reliable diagnostic method for detecting faults. To diagnose transmission defects, random forest models and genetic algorithm-based feature selection were coupled [24]. A support Vector Machine was used for multiclass gearbox diagnosis using interpolation and extrapolation [25]. Bayesian networks are used in the identification of tooth breakage and wear of gears based on statistical parameters obtained from vibration signals[26]. Identification of pitting in gears using scalograms and the mean frequency variation exponent scaling algorithm [27]. However, these methods require professional expertise to use them successfully in diagnosis and are not suitable for automatically detecting the degree of damage in gears. Evaluations of the literature show that the use of knowledgable algorithms, such as Support Vector Machines, ANN, and k-nearest neighbours, can detect defects in machines and enable online and autonomous monitoring. ANN has become more popular than its rivals due to its excellent efficiency in recognising similarities between big data sets; ANN is nothing but the functional imitation of the human brain. Therefore, ANN can make decisions and conclusions even on complex, irrelevant, and noisy data [28]. Notwithstanding the possible non-linearity of the model, results can be obtained within a short time [29]. These features have established ANN as one of the best tools available for defect diagnosis. Recently, Mutra et al. [30,31] explained the use of artificial neural network-based parameter identification and its optimisation in high-speed rotor bearing systems. Mba et al. [32] combined stochastic resonance to amplify weak impulses using noise and hidden Markov modelling (HMM) to model the system observation as a probabilistic function. This is claimed to be a robust diagnostic system but uses only kurtosis and RMS features. Kumar [33] suggested using the power of the Internet of Things (IoT) and deep learning for the next-generation maintenance strategy in condition monitoring. He also advised combining the physical systems with AI models for automatic and efficient vibration-based diagnosis.

The proposed architecture integrates advanced ICT tools with condition-based maintenance to facilitate condition monitoring of the differential gearbox. A systematically developed framework is used to analyse the vibration signals of a differential gearbox using a cloud-based CPS platform. This integrated approach consists of functional modules such as data acquisition, database servers, analysis servers, and reporting modules, which are represented as the physical resource layer, local service layer, and cloud service layer in the proposed framework. The physical resource layer primarily collects various types of input data, gearbox specifications, and operating parameters using different CPS

devices. The collected heterogeneous input data delivered to the data acquisition system (DAQ) in the local service layer is converted into signal data in the time and frequency domains. This data is extracted into feature metrics and stored in the cloud database. This global information is subjected to signal processing by the EMD algorithm. The result is the IMF, which contains the local information of the signal data. This recommended standardised extraction feature can be conveniently adapted for system health monitoring. Synchronisation of the cloud resource layer with the physical resource layer for condition monitoring of the gearbox has not yet been reported. Also, a combination of the EMD potential to convert the signal into IMF with the potential of Euclidian-based distance evaluation technique to identify significant statistical features has not been used for gearbox condition monitoring before. Predicting gear and machinery defects is expensive, both in terms of lost production and repair costs. These errors or losses can lead to the failure of the entire plant or machine. This study aims to replace these losses and defects with predictive maintenance by using advanced machine learning techniques (ML) to detect and predict defects in industrial machinery. Usually, machine components such as gears or cracks wear out after a certain period of operation and early prediction of the damage reduces downtime. This is the great novelty of the present work and a contribution to the condition monitoring of gearboxes in the cement, rubber and plastics industries as well as in power plants. Section 2 of this study describes the tests that were carried out to obtain data on the wear of gears at different running times. Section 3 explains the EMD method, while Section 4 goes into more detail about the features extracted from the signal. Section 5 of this study discusses the results. This study concludes in Section 6 with a forecast for the future.

2.0 PROPOSED ARCHITECTURE

The architecture framework of the cyber-physical system is developed to realise the real-time condition monitoring of differential gearbox. Figure 1 shows the proposed architecture having facilities of the cloud resource layer synced with the physical resource layer. The physical resource layer comprises the gearbox and the transducer (sensor) mounted on it. This cyber-physical system is defined as physical and engineered systems whose operations are monitored, coordinated, controlled, and integrated by a computing and communication core.

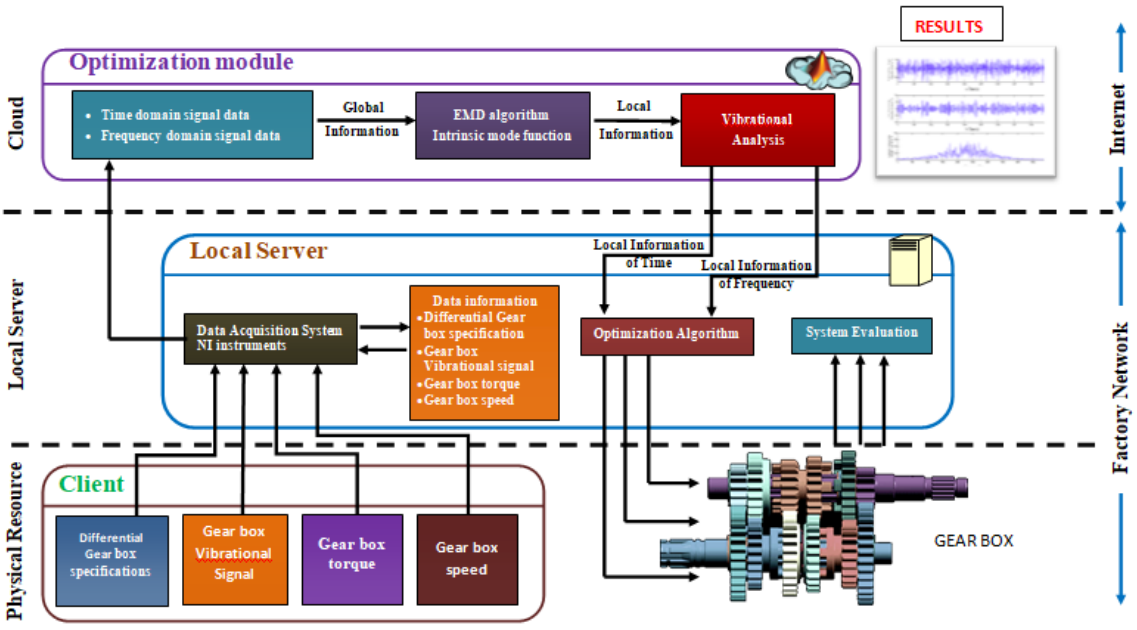

Figure1. The developed architecture of the cloud-based cyber-physical system for condition monitoring of differential gearbox

3.0 EXPERIMENTATION

As shown in Figure 2(a), the established experimental setup aims to collect vibration signal data of the gearbox at different running times. The test setup for the gearbox consists of four gears and an assembly of two parallel shafts. With a module of 4 mm and a pressure angle of 20°, two EN34 steel gears with a total of 50 teeth and two pinions with a total of 25 teeth are used. Table 1 represents the measurements of the gear. The test conditions considered for the current study are shown in Table 2.

A torque limiter is used to connect and hold two shafts on an axle. Gears are mounted on the input shaft and pinions are on the main shafts. A three-phase 10 HP induction motor connected to the driving axle transmits power to the main axle with a reduction ratio 0.7. To introduce the initial torque, a special torque clutch is used, which is clamped with bolts. The bolt heads fit into the T-slots located on the face of one-half of the coupling. This allows clamping together in any relative angular position. Once the clamping bolts are released by holding one half, a lever arm is used to apply torque to the other half. To measure the applied torque, the coupling must be clamped. In a traditional gear test rig, the external load is applied to the gears to apply the torque using a motor and magnetic brake. The motor and magnetic brake must be

controlled at specific and different shaft speeds. A torque clutch keeps the applied torque constant at a specific motor speed while locking the flanges in the shaft loop. This simple and reliable arrangement requires no external load to examine and test the gear system. Figure 2(b) shows the realistic setup of the gearbox. During the tests, the gearbox is run at a speed of 2100 rpm and accelerated test circumstances of 300 Nm and 400 Nm. The applied torque is therefore five times greater than the permissible torque. A B&K 4332 accelerometer installed on the bearing housing is used to measure the vibrations, and a B&K 2626 amplifier amplifies the signals from 0-8 kHz to 16 kHz. No additional amplification was applied as the frequency range obtained intensively reveals the content of the vibration frequency up to about the fifth harmonic of the tooth mesh. The amplified data is stored in the commercial data acquisition system DACTRON (model Focus-100).

Table 1. Specifications of gear

Parameter	Gear	Pinion
Centre distance (mm)	150	
Module (mm)	4	
Width of face (mm)	25	
Diameter of pitch (mm)	200	100
Number of teeth	50	25
Angle of pressure (degree)	20º	
BHN	130	
Modulus of elasticity (N/mm^2)	2×10^5	
Poisson's ratio	0.3	
Type of material used is steel	En 19, 0.22% Carbon	
Modulus of shearG (N/mm^2)	0.8×10^5	
Speed of pinion (rpm)	2100 rpm	
Load in Static condition (kN)	0-0.69 kN	
Armlever L (mm)	600	
Shaft torque of Gear wheel	300 Nm and 400 Nm	

Table 2. Test conditions

Sl. No	Number of hours	Applied torque (Nm)
1	0	300
2	36	300
3	72	300
4	108	300
5	144	300
6	180	300
7	216	300
8	0	400
9	36	400
10	72	400
11	108	400
12	144	400
13	180	400
14	216	400

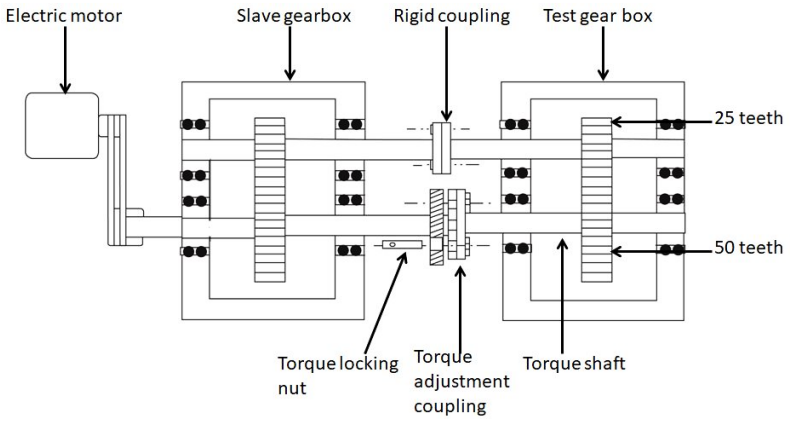

(a) schematic diagram of test rig

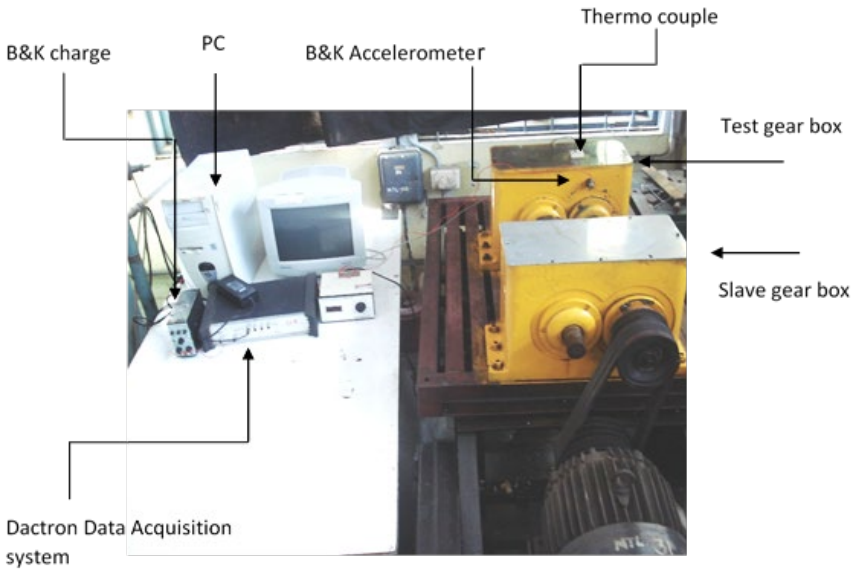

(b) actual test rig

Figure 2. Experimental setup

4.0 EMPIRICAL MODE DECOMPOSITION

The vibrational signal data is divided by empirical mode decomposition (EMD) into several fundamental signals known as IMFs. Since nonstationary, nonlinear signals may be divided into empirical modes, this approach is self-adaptive. These represent the modes of the numerous oscillations that the signal contains. The only element that counts as local information in the EMD algorithm is the IMF, which must be extracted from the original signal. This extraction is carried out using the sifting procedure. Figure 3 shows the flow chart of EMD processing.

The steps of the sifting process are to identify all local maxima and minima for every vibrational data, $x(t)$. All local maxima and minima are connected using cubic splines to create the upper $E_{up}(t)$ and lower $E_{lw}(t)$ envelopes, respectively. The formula for calculating the average of the envelopes is $mean(t)= [E_{up}(t) + E_{lw}(t)]/2$. The formula for calculating the difference between the data and the mean is $d(t)= x(t)-m(t)$. IMF_i is evaluated using the IMF and the stoppage criterion to confirm that the data obtained is an IMF. The above five steps are repeated for $d(t)$ if IMF does not match the conditions of the stoppage criterion. If the conditions for the stoppage criterion are satisfied then $d(t)$ is defined as one more variable $c(t)$. Residue, i.e., $r(t)=x(t)-c(t)$ is calculated by repeating the above seven steps and stored as data. The operation ends when the residue contains more than one extremum.

The stoppage criteria of the filtering phase are a crucial component of the EMD technique. It establishes when the filtering is finished and a new IMF has been discovered. The standard deviation (STD) value serves as the basis for the halting criterion for the sifting process, which is given by

$$STD = \frac{\sum_t \left[d_{(n-1)}(t) - d_{(n)}(t)\right]^2}{\sum_t \left[d_{(n-1)}(t)\right]^2} \quad (1)$$

There are two criteria for ending the sifting process; first if the standard deviation of the IMFs obtained is less than 0.3 (the value considered in this paper), and secondly, when $x(t)$ has only one extreme (since the graph with a single extremes forms a straight line cannot be decomposed further).

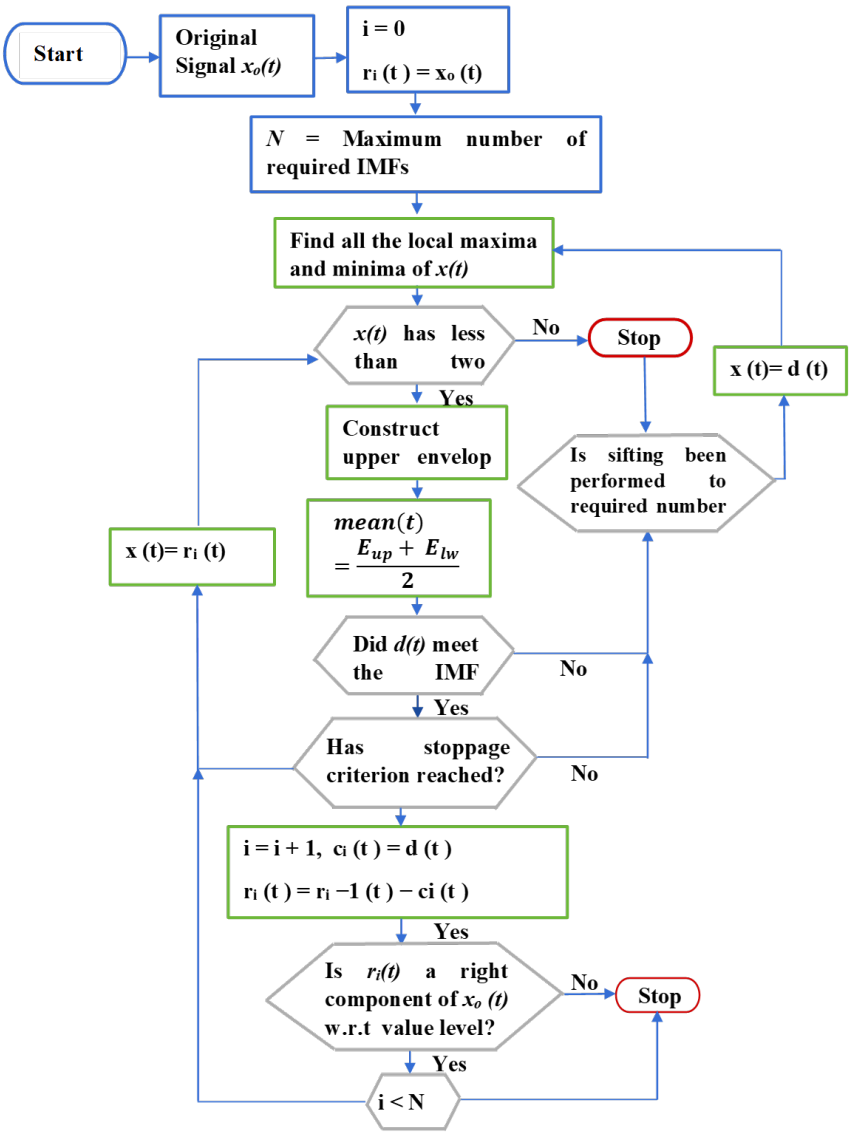

Figure 3. Flowchart of the working of the EMD process

5.0 FEATURE EXTRACTION AND SELECTION

In the experiments conducted, 14 sets of vibrational signals were collected at two different test conditions and seven different runtimes, i.e. from zero to 210 hours runtime with a step size of 36 hours. Throughout the experiment, a constant load was maintained at both accelerated test conditions of 300Nm and 400Nm, using a torque limiter.

5.1 Feature Extraction

Fifteen statistical features were extracted to identify the condition of the fishing gear, and they are divided into two groups; features that span both the temporal and frequency domains. The amplitude of the vibration and signal energy is represented by the root mean square (RMS). Standard deviation (STD) is a term describing the amount of variation from the average value. Root-sum-of-squares (RSSQ) specifies the value of the root sums of the vibration data, summing along the specified dimension; peak value indicates the value of the maximum amplitude in the signal data. Skewness is an indicator of how asymmetrically the data is distributed around the sample mean, and kurtosis is a metric for signal sharpness or the quantity and size of peaks present in the signal. The minimum value provides the minimum value of the signal x, and peak-to-peak returns the difference between the maximum and minimum values in the signal. The crest factor is the maximum positive peak value of the signal divided by RMS. The clearance factor gives the ratio of the maximum absolute value. Shape factor, which may be used to depict the distribution of the time series signal in the time domain. The ratio of the largest absolute value of the signal to its root mean square value (RMS) is known as peak to RMS. The variance coefficient shows how widely the data can be interpreted. It contrasts the standard deviation with the average of the data set. It is determined by the standard deviation to mean ratio. Spectral STD indicates the value of the standard deviation for the signal in the frequency domain. KRMS is the product of the kurtosis value and the corresponding RMS value.

5.2 Feature Selection

Nevertheless, these extracted features help to identify the extent of wear of the gear at different runtimes but not reliable to identify the amount of wear. The sensitivity of some features was found to be closely related to the wear of the gear. Therefore, before the extracted data is fed into the ANN, sensitive features are selected and irrelevant features are discarded or attenuated to improve performance. To identify the significant features, an Euclidean distance evaluation technique based on is used. In the experiments, 14 sets of data were collected for seven different runtimes and two different loading conditions. Fifteen features were extracted for all 14 vibration data sets. Thus, the set of feature values with a 14×2×15 matrix is obtained. The stepwise procedure for identifying sensitive features is as follows. Under the same test conditions, the average distance between samples can be given as follows

$$P_{s,f} = \sqrt{\frac{1}{R_s \times (R_s - 1)} \sum_{s,e=1}^{R_s} \left(A_{m,s,f} - A_{l,s,j}\right)^2}, \ l, m = 1,2, \dots, \ R_s \ l \neq e \tag{2}$$

Now, to get the average distance for both the test conditions S=1,2.

$$P_f^{(w)} = \frac{1}{n} \sum_{s=1}^{R_s} P_{s,f} \tag{3}$$

Finding the variance factor for the same test condition.

$$Var_f^{(w)} = \frac{\max\left(P_{s,f}\right)}{\min\left(P_{s,f}\right)} \tag{4}$$

Average of all the sample feature values under the same test condition.

$$a_{s,f} = \frac{1}{R_s} \sum_{m=1}^{R_s} A_{m,s,f} \tag{5}$$

calculating the samples' average separation under various test conditions:

$$P_f^{(b)} = \sqrt{\frac{1}{S \times (S - 1)} \sum_{s,e=1}^{S} \left(a_{e,f} - a_{s,f}\right)^2}, \ s, e = 1,2, \dots, S, \ s \neq e \tag{6}$$

Finding the variance factor for different test conditions.

$$Var_f^{(b)} = \frac{\max\left(\left|a_{e,f} - a_{s,f}\right|\right)}{\min\left(\left|a_{e,f} - a_{s,f}\right|\right)}, \ s, e = 1,2 \dots, S, \ s \neq e \tag{7}$$

The variance factor can be calculated as follows.

$$\lambda_f = \left(\frac{Var_f^{(w)}}{\max(Var_f^{(w)})} + \frac{Var_f^{(b)}}{\max(Var_f^{(b)})}\right)^{-1} \tag{8}$$

The ratio of $P_f^{(b)}$ and $P_f^{(w)}$ by the factor of λ_f is given by

$$E_f = \lambda_f \frac{P_f^{(b)}}{P_f^{(w)}} \tag{9}$$

Getting the evaluation criteria by normalising E_f.

$$\overline{E}_f = \frac{E_f}{\max\left(E_f\right)} \tag{10}$$

From the above procedure, it is clear that the higher the value $\overline{E}_f$, the more sensitive the feature. Thus, all the features $\overline{E}_f \geq \mu$ are selected for further procedures. Where μ is the pre-defined threshold value. The entire methodology proposed for diagnosis is represented in Figure 4. The artificial intelligence model is fed both the most sensitive features and all features, and the performance of the model is compared to confirm the selection of features. For the final diagnosis, the results of the feature selection are compared.

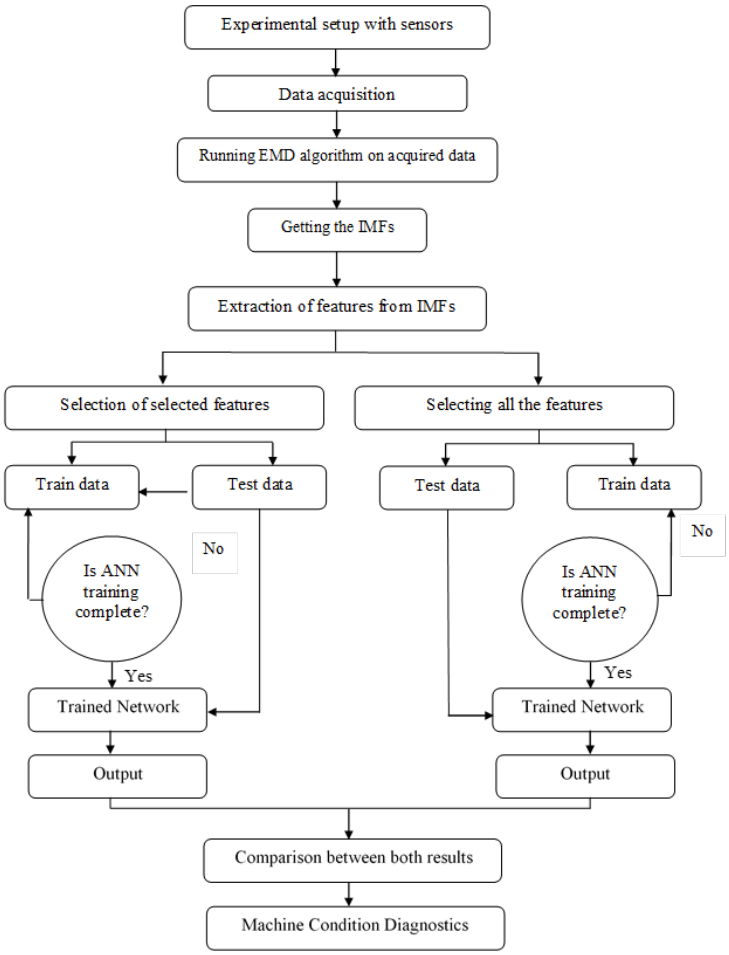

Figure 4. Proposed methodology

6.0 RESULTS AND DISCUSSION

6.1 Experimental Results

The experimental setup was carried out under different test conditions, and the data was extracted and processed. Figure 5(a) and 5(b) show the raw signal in the time domain for the test conditions of zero hours and 36 hours at 300 Nm applied torque. Furthermore, the EMD algorithm was applied to these raw signals in the time domain to obtain the first three IMFs, as shown in Figure 6(a) and 6(b).

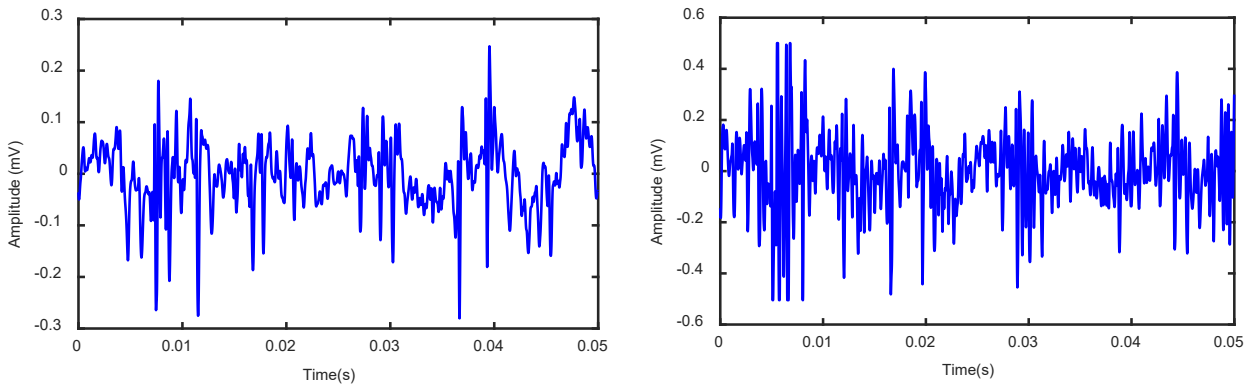

(a) Zero-hour runtime (b) 36 hours runtime

Figure 5. Raw signal in the time domain at two conditions for 300 N-m applied torque

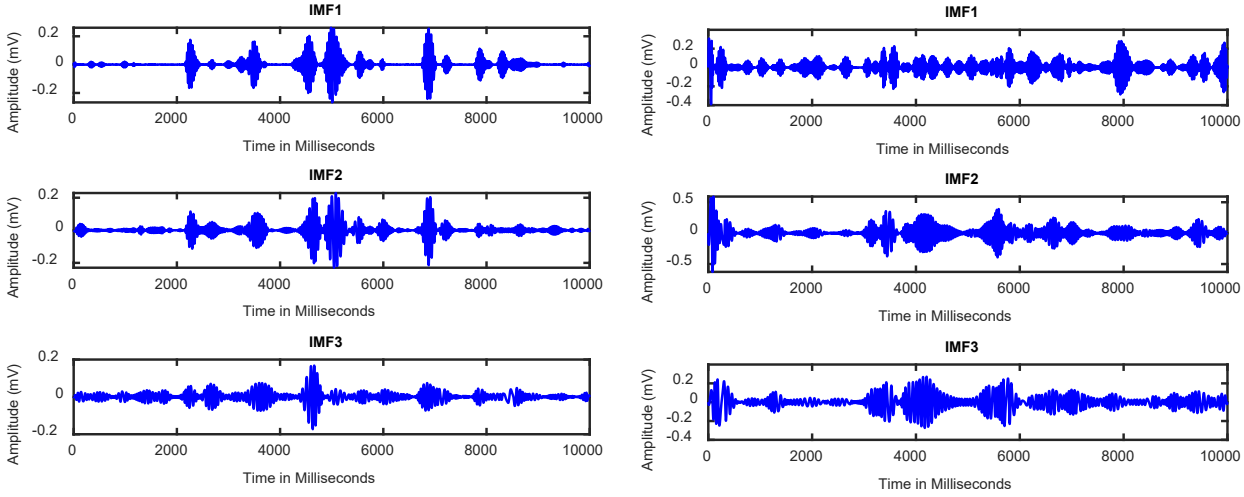

(a) Zero-hour runtime (b) 36 hours runtime

Figure 6. IMFs 1, 2, and 3 of Time-domain signal at two conditions for 300 N-m torque applied

It can be observed that the changes in the time domain in each IMF are compared to the raw signal. In addition, the frequency response of the system was evaluated under the same conditions at 0 hours and 36 hours of operation at 300 Nm. The frequency response of the system for run times of 0 and 36 hours is shown in Figure 7.

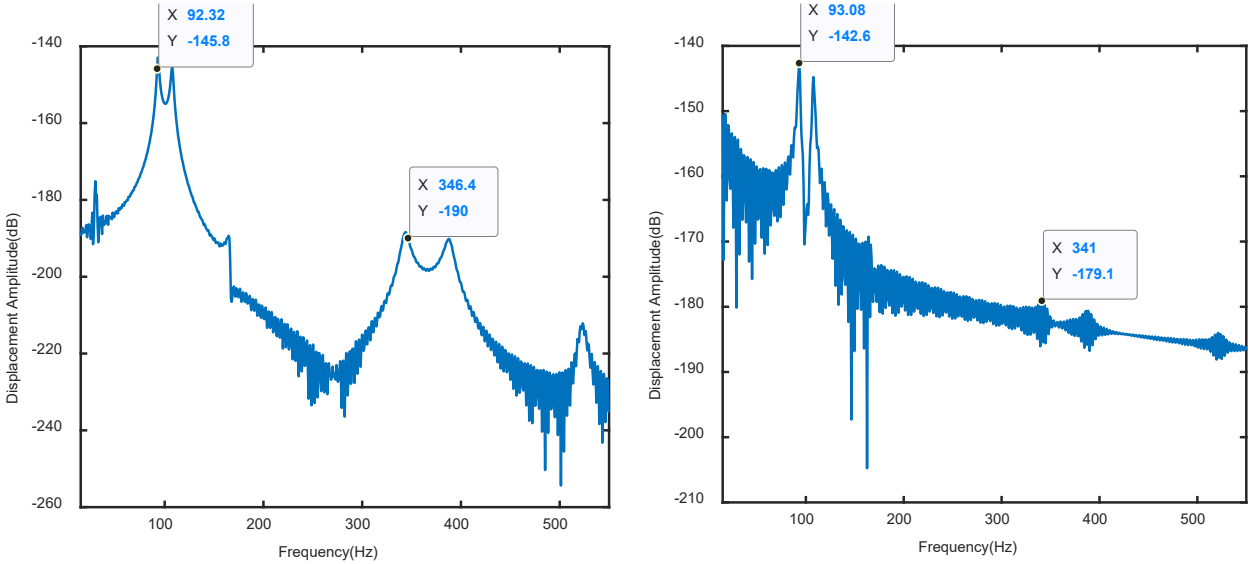

(a) FFT zero-hour runtime (b) FFT 36-hour run time

Figure 7. Frequency response signal at two conditions for 300 N-m torque applied

It can be observed that the first peak frequency in both cases is 92.32 Hz and 93.08 Hz, but the signal converges more at a run time of 36 hours, and the peaks come very close. This may be due to the runtime hours of the system. Figure 8 shows the raw time domain signal for two test conditions at 0 hours and 36 hours of operation at 400 Nm. Figure 9(a) and 9(b) show the first three IMFs for the raw signals in the time domain obtained in two test conditions at applied torque 400 N-m. Later, in the experiments conducted, 14 sets of vibrational signals were collected at two different test conditions and seven different runtimes, i.e. from zero-hour runtime to 210-hour runtime with a step size of 36 hours. Throughout the experiment, a constant load was maintained at both accelerated test conditions, i.e. 300 Nm and 400 Nm, by using a torque limiter. Figure 10 shows the ten most sensitive statistical parameters determined from the vibration response at the two test conditions, 300 N-m and 400 N-m.

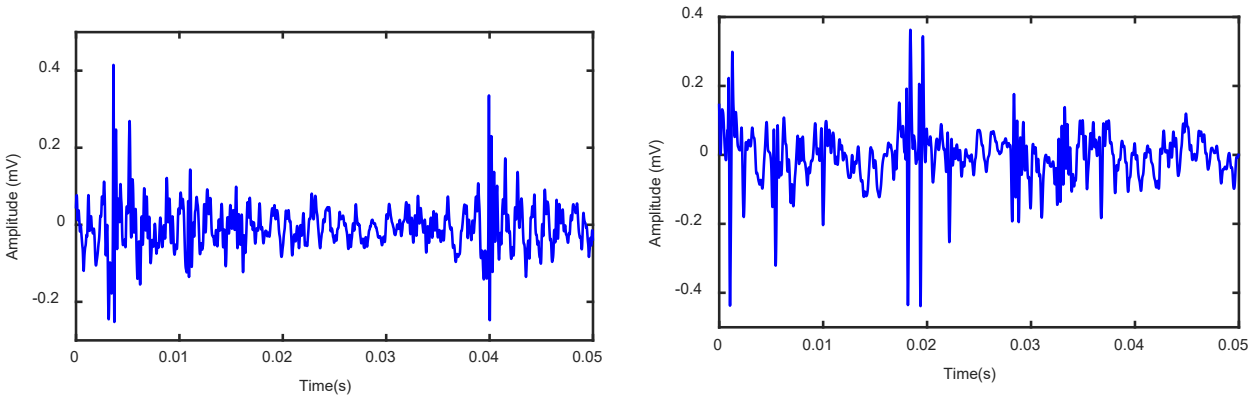

(a) Zero-hour runtime (b) 36 hours runtime

Figure 8. Time-domain raw signal at two conditions for 400 N-m torque applied

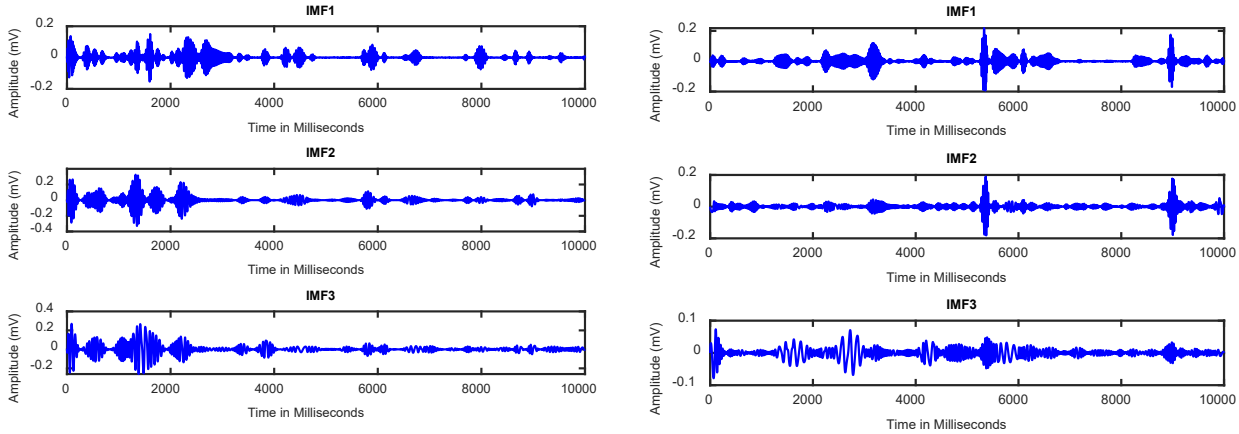

(a) Zero-hour runtime (b) 36 hours runtime

Figure 9. IMFs 1, 2, and 3 of Time-domain signal at two conditions for 400 N-m torque applied

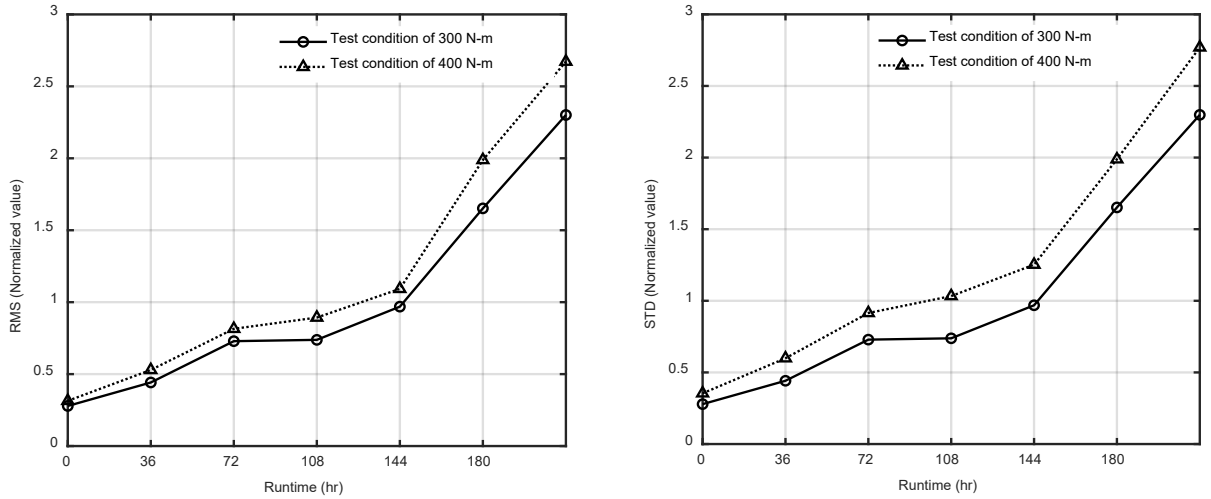

(a) RMS (b) STD

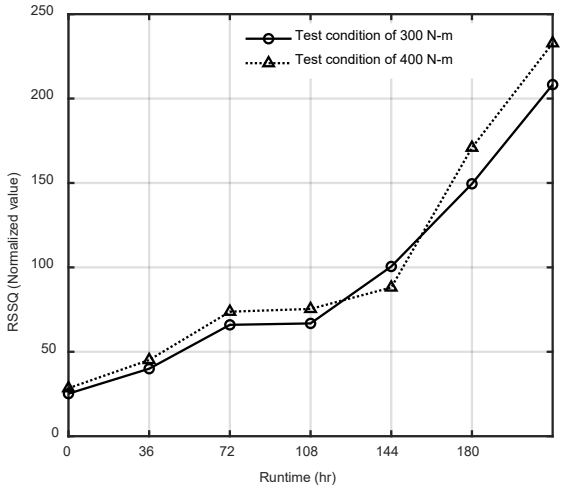

(c) RSSQ

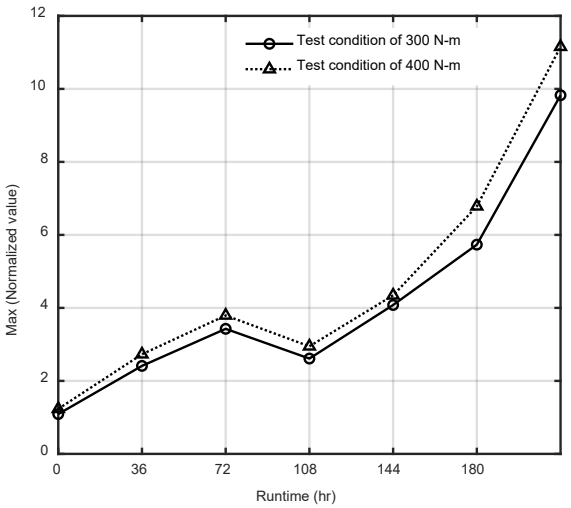

(d) max

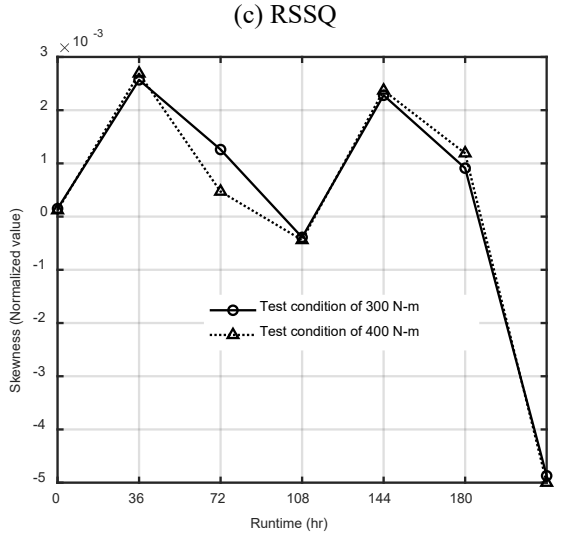

(e) Skewness

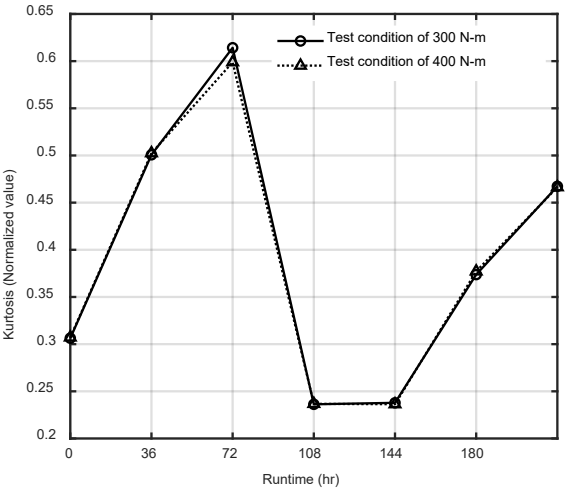

(f) Kurtosis

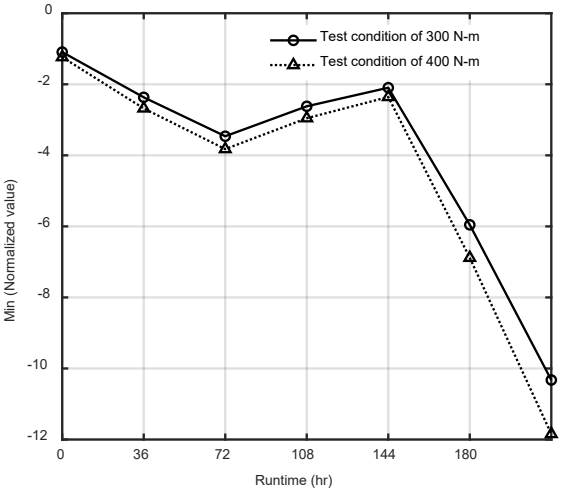

(g) Min

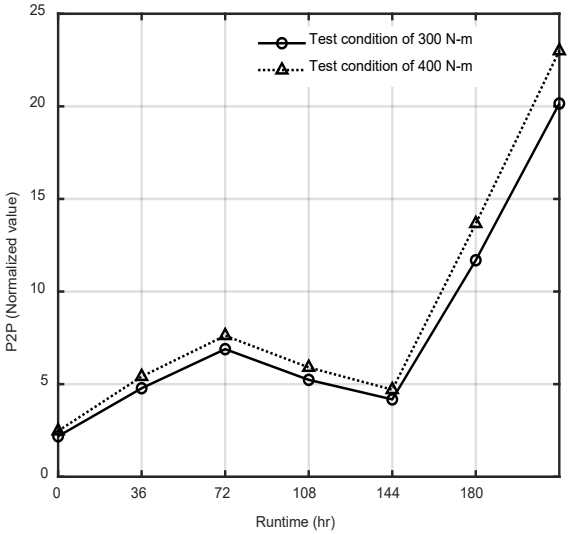

(h) P2P

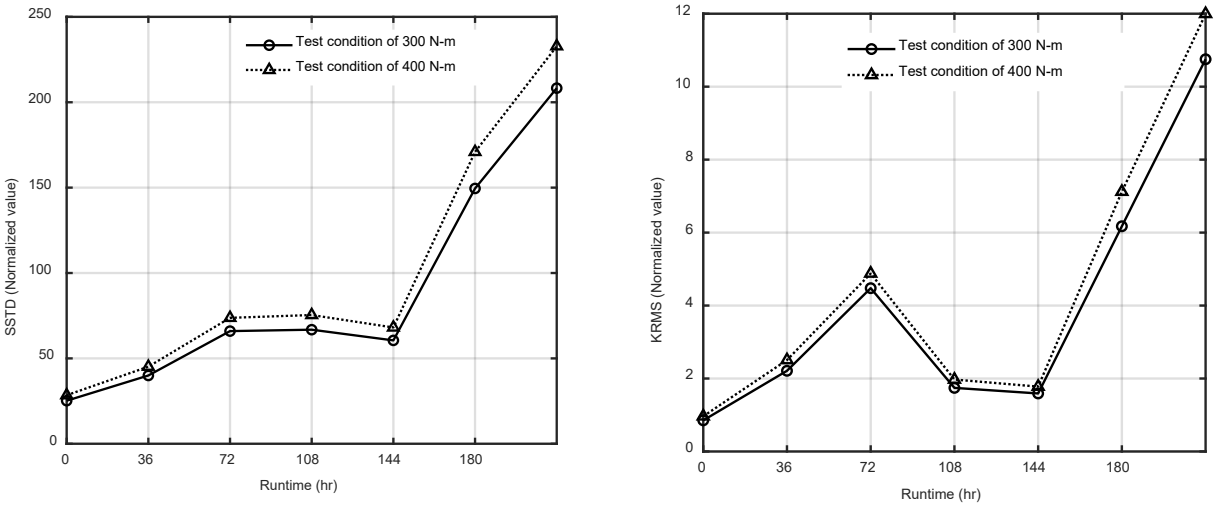

(i) SSTD (j) KRMS

Figure 10. Statistical parameters at two test conditions of 300N-m and 400 N-m

It can be observed that RMS, STD, RSSQ, Max, P2P, SSTD, and KRMS show a pattern of increasing IMF values with increasing runtime and follow a certain trend. Each detected vibrational signal is processed to extract these features. Therefore, a range of feature values determined by $\{A_{r,s,f}\ r=1,2...R,\ s=1,2...S,\ f=1,2...F\}$, the R-by-S-by-F matrix can be detected. Where $A_{r,s,f}$ the f^{th} feature is under the r^{th} sample of the s^{th} condition, f is the number of features, S is the number of test conditions, and R is the total number of runtimes (samples). In this work, R is 14, S is 2 and F is 15. Figure 11 shows the results of the evaluation criteria for feature selection. The features that are above the threshold have the most potential and are, therefore selected for further monitoring. These features are the most sensitive to gear wear. Here the solid line indicates the 300 N-m test condition, and the dotted line indicates the 400 N-m test condition.

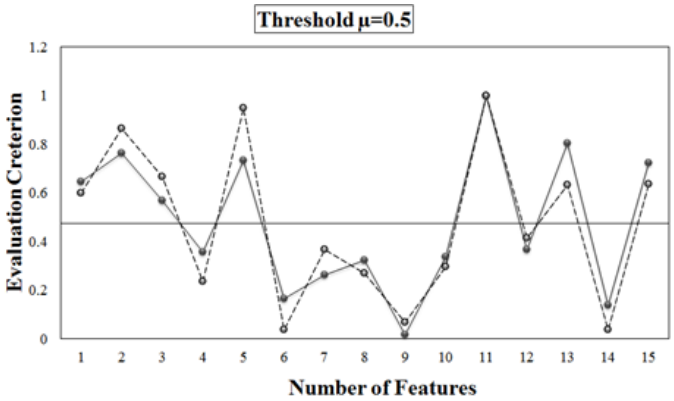

Figure 11. Evaluation criteria for all ten features

6.2 Artificial Neural Network

Neural networks function similarly to the human brain, especially in processing. They need to be fed some test data to categorise or already have a definite answer. Based on this data, they adjust their values using backpropagation algorithms to form a network that predicts the answer based on further input. This comes in different sizes and shapes that can be adapted to the processing power of computers. It is relatively efficient in various technical areas where a pattern needs to be recognised in a large amount of data. The BPNN and the RBF were the two types of neural networks used in the current study. Figure 12 shows the architecture of a multilayer neural network with backpropagation and feedforward.

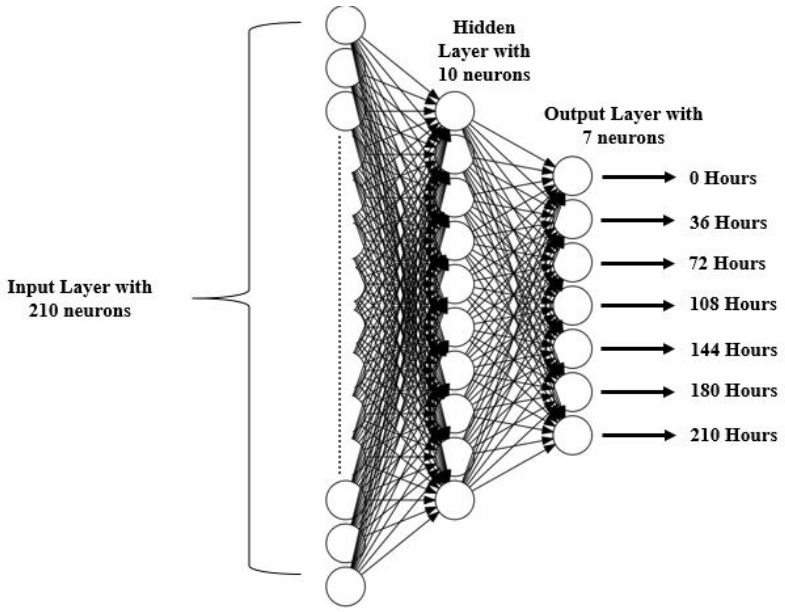

Figure 12. Multilayer ANN

The collected features of the signal are used as input to the structure, which has 15 node inputs. The output is a single node that indicates the number of hours the gearbox has been in operation. There is another hidden layer that consists of 10 nodes and is directly connected to the output and input layers. The activation function for initialisation is the tan-sigmoidal (tanh) function, and the sigmoidal (log-sigmoid) is the transfer function for transferring values between the hidden and output layers. The network uses the Levenberg-Marquardt algorithm to optimise the hidden layers. A standard division of 70% in training and 15% each in testing was used to validate the algorithm. The algorithm uses an iterative method to optimise its biases after each epoch and to maximise the validation performance after each iteration. The training process is continued until a certain convergence is no longer reached.

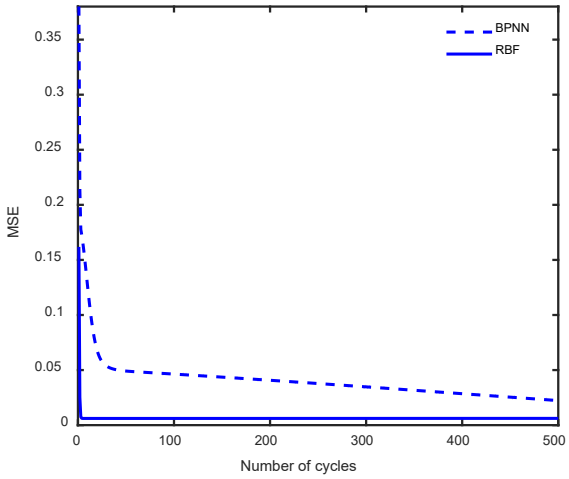

Figure 13. Convergence plot of trained data with all features

Figure 13 shows the convergence plot of the network used after training for both BPNN and RBF. It can be observed that the convergence of RBF is faster compared to BPNN and has a lower MSE. The convergence plot with a good gradient shows a good fit for the data. The lower value of MSE shows that the network is trained properly with a sufficient number of iterations. The downward gradient of the slope shows that the value is much more general and eliminates the probability of overfitting the data. The trained network was also tested with all the previous data after full implementation to get an estimate of its accuracy. The data obtained showed that the MSE was around 0.02, indicating that the network performs with very good accuracy. During feature selection, all extracted features were categorised to select the most optimal features. In addition, the values of the selected features were used for training the neural network with the same dimensions to achieve better results.

Figure 14 shows the convergence plot of the network used after training for both BPNN and RBF. It can be observed that RBF converges much faster compared to BPNN and compared to the previous case, the net MSE error decreases slightly in the present case. However, the slope of the error smoothed out significantly when uncorrelated features were removed. The number of epochs also dropped dramatically, showing that the algorithm works much faster with the

selected features than with all features. The overall test with the entire data in the neural network resulted in an MSE of about 0.005, which is some improvement over the previous data set with all features.

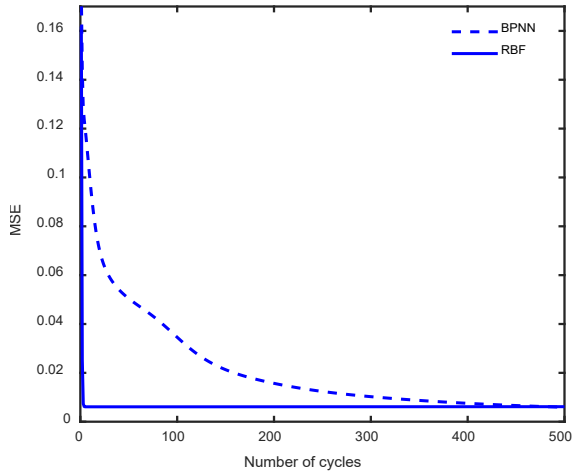

Figure 14. Convergence plot of trained data with selected five features

7.0 CONCLUSIONS

The advantage of distributed resources is that they enable systems to make robust decisions by analysing large amounts of information and sharing data in real time. Experiments were conducted with an industrial differential gear to collect time-domain data of vibration signals at various time periods from 0 to 210 hours at 36-hour intervals. This data, which contained information about the wear of the gearbox, was processed using the EMD algorithm to obtain the most sensitive signals. Ten features in the time and frequency domain were extracted from the processed data (IMF). From the ten extracted statistical parameters of gear wear, the five most sensitive features were selected using the Euclidean distance-based evaluation technique. The dataset was used to train an ANN, and the results of the training were compared with all the extracted features and performance. The results of ANN showed that the proposed strategy significantly increases the performance of the network and reduces the computation time. The present method is particularly promising when the data set is very large, such as in the process industry. This advantage can reduce the cost that the industry spends on storing the data in the cloud platform and reduce the need for powerful servers to perform complex computations. Below are some concluding remarks

i. Three IMFs were predicted from the time domain signal at two conditions: zero run time and 36 hours run time. As the run time increased, the wear rate increased, which can be seen from the shift in the signal. With increasing runtime, additional peaks formed in the frequency response, a behaviour that can be attributed to the wear of the gearbox
ii. The most sensitive element of the vibration response was determined and served as input for an artificial neural network.
iii. Convergence was tested using two ANN techniques: the neural backpropagation network and the radial basis function. It was found that the RBF network converged much faster and required less time to compute than the BPNN.
iv. The selected features provided some improvements over the previous dataset with all features.
v. The present method is promising, especially when the dataset is very large, such as in the process industry. This can reduce the cost the industry spends on storing the data in the cloud platform and reduce the requirement for powerful servers to perform complex computations.

8.0 ACKNOWLEDGEMENT

The Vellore Institute of Technology in Vellore, Tamil Nadu, India, and Universiti Teknologi MARA (UiTM), Shah Alam, Malaysia, provided the research facilities required for this work, for which the authors are grateful. The Vellore Institute of Technology, Vellore, Tamil Nadu, India, and Universiti Teknologi MARA (UiTM), Shah Alam, Malaysia funded this work through the VIT- International Research Fund Scheme (VIN), award number: VIN /2022-23/002, and Strategic Research Partnership (SRP), Award number: 100-RMC 5/3/SRP (086/2022).

9.0 REFERENCES

[1] R. Rajkumar, I. Lee, L. Sha, and J. Stankovic, "Cyber-physical systems: The next computing revolution," In Proceedings of the 47th Design Automation Conference, 2010, pp. 731–736.
[2] J. Manyika, M. Chui, P. Bisson, J. Woetzel, R. Dobbs, *et al.*, "The internet of things: mapping the value beyond the hype," 2015, [Online]. Available: https://apo.org.au/node/55490 [Accessed October 31, 2022].

[3] K. Liu, P. Zhong, Q. Zeng, D. Li, and S. Li, "Application modes of cloud manufacturing and program analysis," *Journal of Mechanical Science and Technology*, vol. 31, pp. 157–164, 2017.
[4] J. Lee, H.D. Ardakani, S. Yang, and B. Bagheri, "Industrial big data analytics and cyber-physical systems for future maintenance & service innovation," *Procedia CIRP*, vol. 38, pp. 3–7, 2015.
[5] J. Shi, J. Wan, H. Yan, and H. Suo, "A survey of cyber-physical systems," In 2011 International Conference on Wireless Communications and Signal Processing (WCSP), 2011, pp. 1–6.
[6] F. Elasha, C. Ruiz-Cárcel, D. Mba, G. Kiat, I. Nze, and G. Yebra, "Pitting detection in worm gearboxes with vibration analysis," *Engineering Failure Analysis*, vol. 42, pp. 366–376, 2014.
[7] B. Van Hecke, J. Yoon, and D. He, "Low speed bearing fault diagnosis using acoustic emission sensors," *Applied Acoustics*, vol. 105, pp. 35–44, 2016.
[8] T. Touret, C. Changenet, F. Ville, M. Lalmi, and S. Becquerelle, "On the use of temperature for online condition monitoring of geared systems – A review," *Mechanical Systems and Signal Processing*, vol. 101, pp. 197–210, 2018.
[9] Y. Gritli, A. Bellini, C. Rossi, D. Casadei, F. Filippetti, and G.-A. Capolino, "Condition monitoring of mechanical faults in induction machines from electrical signatures: Review of different techniques," IN 2017 IEEE 11th International Symposium on Diagnostics for Electrical Machines, Power Electronics and Drives (SDEMPED), 2017, pp. 77–84.
[10] S. Sheng, "Monitoring of wind turbine gearbox condition through oil and wear debris analysis: A full-scale testing perspective," *Tribology Transactions*, vol. 59, pp. 149–162, 2016.
[11] N. Ullah, T. Cong, B. Huan, and H. Yucheng, "Influence of optimal tooth modifications on dynamic characteristics of a vehicle gearbox," *International Journal of Automotive and Mechanical Engineering*, vol. 16, pp. 6319–6331, 2019.
[12] X. Fan, and MJ Zuo, "Gearbox fault detection using Hilbert and wavelet packet transform," *Mechanical Systems and Signal Processing*, vol. 20, pp. 966–982, 2006.
[13] J. Chen, Z. Li, J. Pan, G. Chen, Y. Zi, *et al.*, "Wavelet transform based on inner product in fault diagnosis of rotating machinery: A review," *Mechanical Systems and Signal Processing*, vol. 70–71, pp. 1–35, 2016.
[14] F. Duan, F. Elasha, M. Greaves, and D. Mba, "Helicopter main gearbox bearing defect identification with acoustic emission techniques," In 2016 IEEE International Conference on Prognostics and Health Management (ICPHM), 2016, pp. 1–4.
[15] N.E. Huang, Z. Shen, S.R. Long, M.C. Wu, H.H. Shih, *et al.*, "The empirical mode decomposition and the Hilbert spectrum for nonlinear and nonstationary time series analysis," *Proceedings of the Royal Society of London. Series A: Mathematical, Physical and Engineering Sciences*, vol. 454, pp. 903–995, 1998.
[16] M.C. Peel, T.A. McMahon, and G.G.S. Pegram, "Assessing the performance of rational spline-based empirical mode decomposition using a global annual precipitation dataset," *Proceedings of the Royal Society A: Mathematical, Physical and Engineering Sciences*, vol. 465, pp. 1919–1937, 2009.
[17] S.J. Loutridis, "Damage detection in gear systems using empirical mode decomposition," *Engineering Structures,* vol. 26, pp. 1833–1841, 2004.
[18] M.R. Reddy, and J. Srinivas, "Vibration analysis of a support excited rotor system with hydrodynamic journal bearings," *Procedia Engineering*, vol. 144, pp. 825–832, 2016.
[19] B. Samanta, "Gear fault detection using artificial neural networks and support vector machines with genetic algorithms," *Mechanical Systems and Signal Processing*, vol. 18, pp. 625–644, 2004.
[20] P. Melin, "Analysis and design of intelligent systems using soft computing techniques," [Online]. Available: https://link.springer.com/book/10.1007/978-3-540-72432-2 [Accessed October 31, 2022].
[21] I.A. Abu-Mahfouz, "A comparative study of three artificial neural networks for the detection and classification of gear faults," *International Journal of General Systems*, vol. 34, pp. 261–277, 2005.
[22] L. Wuxing, P.W. Tse, Z. Guicai, and S. Tielin, "Classification of gear faults using cumulants and the radial basis function network," *Mechanical Systems and Signal Processing*, vol. 18, pp. 381–389, 2004.
[23] Y. Lei, and M.J Zuo, "Gear crack level identification based on weighted K nearest neighbour classification algorithm," *Mechanical Systems and Signal Processing*, vol. 23, pp. 1535–1547, 2009.
[24] M. Cerrada, G. Zurita, D. Cabrera, R.-V. Sánchez, M. Artés, and C. Li, "Fault diagnosis in spur gears based on genetic algorithm and random forest," *Mechanical Systems and Signal Processing*, vol. 70–71, pp. 87–103, 2016.
[25] S. Bansal, S. Sahoo, R. Tiwari, and D.J. Bordoloi, "Multiclass fault diagnosis in gears using support vector machine algorithms based on frequency domain data," *Measurement*, vol. 46, pp. 3469–3481, 2013.
[26] H. Öztürk, M. Sabuncu, and I. Yesilyurt, "Early detection of pitting damage in gears using mean frequency of scalogram," *Journal of Vibration and Control*, vol. 14, pp. 469–484, 2008.
[27] R.R. Schoen, B.K. Lin, T.G. Habetler, J.H. Schlag, and S. Farag, "An unsupervised, online system for induction motor fault detection using stator current monitoring," *IEEE Transactions on Industry Applications*, vol. 31, pp. 1280–1286, 1995.
[28] S.I. Hoodorozhkov, A.A. Krasilnikov, and M.S. Gubachev, "Optimisation of an algorithm for automatic control of transmission in a wheeled tractor," *International Journal of Automotive and Mechanical Engineering*, vol. 18, pp. 9051–9060, 2021.
[29] B.S. Yang, T. Han, and JL An, "Art–Kohonen neural network for fault diagnosis of rotating machinery," *Mechanical Systems and Signal Processing*, vol. 18, pp. 645–657, 2004.
[30] R.R. Mutra, and J. Srinivas, "An optimisation-based identification study of cylindrical floating ring journal bearing system in automotive turbochargers," *Meccanica,* vol. 57, pp. 1193–1211, 2022.
[31] R.R. Mutra, J. Srinivas, and R. Rządkowski, "An optimal parameter identification approach in foil bearing supported high-speed turbocharger rotor system," *Archive of Applied Mechanics,* vol. 91, pp. 1557–1575, 2021.
[32] C.U. Mba, V. Makis, S. Marchesiello, A. Fasana, and L. Garibaldi, "Condition monitoring and state classification of gearboxes using stochastic resonance and hidden Markov models," *Measurement*, vol. 126, pp. 76–95, 2018.
[33] A. Kumar, C.P. Gandhi, Y. Zhou, R. Kumar, and J. Xiang, "Latest developments in gear defect diagnosis and prognosis: A review," *Measurement*, vol. 158, p. 107735, 2020.